 doi:10.20944/preprints202106.0268.v1

Article

Therapeutic potential of human neural precursor cells in diabetic retinopathy – Preclinical model

Claudia S. Saçaki [1], Bassam F. Mogharbel [1], Priscila E. F. Stricker [1], Dilcele S. M. Dziedzic [1], Ana C. Irioda [1], Maiara C. Perussolo [1], Fabiano Montiani-Ferreira [2], Juan Moreno [2], Peterson Dornbusch [2], Mário Sato [3], Naoye Shiokawa [3], Lúcia Noronha [4], Seigo Nagashima [4], Marianna Bacellar-Galdino [5], Célia Regina C. Franco [6], Eltyeb Abdelwaid [7] and Katherine A. T. Carvalho [1*]

[1]Advanced Therapy and Cellular Biotechnology in Regenerative Medicine Department, The Pelé Pequeno Príncipe Research Institute, Child and Adolescent Health Research & Pequeno Príncipe Faculties, Ave. Silva Jardim, 1632, Box: 80.240-020. Curitiba, Paraná, Brazil;
[2]Veterinary Medicine Department, Federal University of Paraná, Rua dos Funcionários, 1540, Box: 80035-050. Curitiba, Paraná, Brazil.
[3]Ophthalmology Department, Federal University of Paraná, Rua Padre Camargo, 285, Box: 80060-240. Curitiba, Paraná, Brazil
[4] Pathology Laboratory of Institute of Biological and Health Sciences of Pontifical Catholic University of Paraná (PUCPR), Street Imaculada Conceição, 1155, Box 80.215-901. Curitiba, Paraná, Brazil;
[5]Ophthy-DS, Bobwhite Ave Kalamazoo, 5512, Box: 49.009. Michigan, USA.
[6]Molecular Biology Department, Federal University of Paraná, Ave. Cel. Francisco H. dos Santos, 100, Box: 81531-980. Curitiba, Paraná, Brazil.
[7]Feinberg School of Medicine, Feinberg Cardiovascular Research Institute, Northwestern University, 303 E. Chicago Ave. Tarry 14–725, Box: 60611. Chicago, IL, USA.

*Correspondence: katherinecarv@gmail.com; Phone: +55-41-3310-1719

Abstract: This study aimed to evaluate cell therapy with human neural precursor cells (hNPCs) in diabetic retinopathy (DR) Wistar rats, induced to diabetes by intraperitoneal injection with streptozotocin. Wharton's Jelly Mesenchymal stem cells (WJ-MSCs) were isolated, expanded, and seeded onto a biopolymer substrate without growth factors to develop neurospheres to obtain the hNPCs, characterized by immunocytochemistry. The animals were divided into three groups; non-diabetic (ND) n = four; diabetic without treatment (DM) n = nine; and diabetic with cell therapy (DM + hNPCs) n = nine. After eight weeks of diabetes induction and verified DR, intravitreal injection of hNPCs (1 x 10^6 cel/µL) was performed in the DM + hNPCs group. Optical Coherence Tomography (OCT) and Electroretinography (ERG) evaluations were done before and after diabetes induction and after cell therapy. Eye enucleation occurred four weeks after treatment for the histopathological and immunohistochemistry analyses. In the treated group, there was the repair of the retinal structures and their arrangements. hNPCs increased the thickness of neuroretina layers, especially in the ganglion cell and photoreceptor layers. The results indicate that hNPCs reduced DR progression by a neuroprotective effect and promoted retinal repair, making them potential candidates for regeneration of the neuroretinal tissue.

Keywords: diabetic retinopathy; mesenchymal stem cells; neural precursor cells; stem cell.

Preprints (www.preprints.org) | NOT PEER-REVIEWED | Posted: 9 June 2021 doi:10.20944/preprints202106.0268.v1

1. Introduction

Diabetic retinopathy (DR) is one of the complications of *Diabetes mellitus* (DM), resulting in decreased visual acuity and impairment that causes blindness [1, 2]. Considering the high number of individuals diagnosed with Diabetes and are suffering its consequences, medicines, treatments, and research have been done to achieve DR long-awaited regression and cure.

Hyperglycemic control can reduce or slow down the progression of DR, but the lack of it contributes to the apoptosis of endothelial cells and neurons through toxicity [3]. Chronic hyperglycemia is accompanied by early dysregulation of mechanisms in the entire retinal neurovascular complex, with neuronal apoptosis and vascular abnormalities in the retina [4, 5, 6]. This chronicity induces several changes, including a proinflammatory state causing hypoxia in the retina [7].

Many signs can be observed during DR progression, from the non-proliferative stage (e.g., inflammation, loss of pericytes, neuronal cells, microvascular disorder) to the proliferative one (e.g., ischemia, neovascularization) [8, 9], and no perfusion capillary as an irreversible vascular process [9].

Retina has a complex network; to function correctly, an intimate coupling between neuronal and vascular processes of this tissue is necessary. This heterogeneous composition is responsible for maintaining the homeostasis, neuroprotection and immune response, performed through glial cells, resident microglia, and the interaction in the retina environment [10]. Initially, Müller cells activation protects the retina from hyperglycemia-induced stress; however, chronic inflammation promotes Müller cell proliferation, resulting in cytotoxic gliosis and increased neural cell death [10]. All disorders caused by Diabetes disrupt the communication between neurons and glia [11].

DR was first characterized as microvascular disease, but it was evidenced to a different approach, that vascular abnormalities with Blood Retinal Barrier (BRB) breakdown are interdependent to neural apoptosis, disrupting the neuroretinal complex, involving many retinal cell types [5]. The establishment and progression of DR can be verified through clinical and image exams, observing morphology and vascular anomalies by Topical Endoscopy Fundus Imaging (TEFI) and Optical Coherence Tomography (OCT) and, also Electroretinography (ERG), which demonstrates the response to electrical stimuli from the retina, reduced in the diabetic retina [12, 13].

Studies with mesenchymal stem cells (MSCs) have been promising, demonstrating effects on neuroprotection, regeneration, and triggering the release of growth factors and cytokines [14, 15], also the immunoreactive for nestin, a protein that marks neural stem cells (NSC)/progenitor cell [16]. Umbilical-cord Wharton´s jelly (WJ) is an excellent source of MSCs, which also demonstrated the ability to differentiate into NSC under the influence of specifics growth factors in vitro [15, 17, 18]. The ease of obtaining these cells and their biological characteristics reinforce their application in studies and clinical treatments.

WJ-MSCs were chosen because they enabled obtaining neural precursor cells (NPCs), an undifferentiated lineage of neural stem cells. In the NPC, both cell populations were observed: the mesenchymal stem cells and neural stem cells [16, 19]. For cell therapy treatment, these cells seem to have the characteristics closest to the objective of improving or repairing the retina, a virtually neuronal tissue. This study aimed to evaluate the treatment for DR with human neural precursor cells (hNPCs) in a preclinical rodent model.

2. Materials and Methods

2.1. Ethics

The human umbilical cord sample was collected after the Research Ethics Human Committee of Pequeno Príncipe Faculties authorization (Approval number 3.288.297 - 2019) at the Hospital Maternidade Victor Ferreira do

Preprints (www.preprints.org) | NOT PEER-REVIEWED | Posted: 9 June 2021 doi:10.20944/preprints202106.0268.v1

Amaral (Curitiba, Brazil). The animal study was approved by the Pequeno Príncipe Faculty Animal Ethics Committee (Approval number 041-2018), and all experiments were performed following the ARRIVE Guidelines [20]. *Rattus norvegicus* – male Wistar were divided into three groups, non-diabetic, ND (n = 4), diabetic, DM (n = 9), and diabetic with cell therapy, DM+hNPCs (n = 9), with water and standard diet *ad libitum*.

2.2. Isolation of WJ-MSCs

WJ-MSCs from one umbilical cord, isolated from explant method, were placed in a standard medium with Dulbecco's Modified Eagle Medium: Nutrient Mixture F-12 (DMEM Ham F-12, Sigma-Aldrich®), supplemented with 20% fetal bovine serum (FBS, Gibco®), 100 IU/mL penicillin, and 0.1 mg/mL streptomycin (Gibco®); incubated at 37 °C, 5% CO2 atmosphere [15].

After cell migration from small tissue fragments to the dish surface, cells were detached through 0.25% trypsin enzymatic digestion (Sigma-Aldrich®), plated at a density of 1 x 10^4 cells/cm^2, and the medium was changed twice a week until reaching confluence [21]. Cell samples were differentiated to confirm trilineage potential, and immunophenotyping was made by flow-cytometry analysis [22]. Monoclonal antibodies against cell surface markers CD105 / CD73 (BD Pharmingen®), CD90 (eBioscience®), HLA-AB, CD34 / CD45, and HLA-DR (Biolegend®) antigens were detected by fluorescence. Cell viability evaluation was performed with a 7-Aminoactinomycin D (7-AAD) marker. These analyses were performed in triplicates [23].

2.2.1. Induction of hNPCs

WJ-MSCs resuspended in 20 µL of the standard medium at 1 x 10^4 cell concentration was deposited in the center of each well, as a micromass seeded on a biopolymer substrate polyisoprene-based, and incubated for 20 min before 500 µL of a standard medium was added in each well. The standard medium was changed twice a week [24]. The development of several agglomerated cell spheres was observed after one week, and the neurospheres were identified. Neurospheres were removed from the substrate through mechanical detachment, dissociated by trypsin, and seeded at 1 x 10^5 cells/cm^2 on cell culture flasks to reach 80% cell confluence [15]. At this phase, hNPCs were formed and could be used for transplant. To the aim of identifying neural markers after neurosphere formation, the culture medium was removed, cells were fixed with 2% paraformaldehyde (Sigma-Aldrich®), and washed with phosphate buffer saline (PBS, Thermo Fisher®), before permeabilization with Triton (Amresco®). The culture was incubated with primary antibodies anti-nestin and anti-β-III tubulin (Sigma- Aldrich®) overnight at 4°C, washed and incubated with the secondary antibody anti-rabbit Alexa Fluor 488 (Invitrogen®), followed by Hoechst 33258 (Invitrogen®)[25].

2.3. DR development and in vivo evaluations of diabetes

2.3.1 Diabetes induction

Diabetes induction was made with an intraperitoneal injection (ip) of streptozotocin (STZ, Sigma- Aldrich®) (65 mg/kg) on 180g rats from DM and DM+hNPCs groups, using the protocol from the Unit for Laboratory Medicine Guidelines and Standard Operating Procedures [26], followed by 10% sucrose water drink supplementation for 48 h.

Preprints (www.preprints.org) | NOT PEER-REVIEWED | Posted: 9 June 2021 doi:10.20944/preprints202106.0268.v1

Blood glucose level was measured once a week with a glucometer (Accu-chek® Performa, Roche) to certify hyperglycemia, and ⩾ 200 mg/dL was considered diabetic.

2.3.2. Electroretinography (ERG) and Topical Endoscopy Fundus Imaging (TEFI)

Animals were anesthetized with isoflurane by inhalation with oxygen support to perform TEFI and electroretinogram (ERG) exams, using one drop of 1% tropicamide (Alcon) in each eye. TEFI was executed with a 3 mm diameter rigid probe and a 175W xenon lamp connected to a digital reflex camera (7.2-megapixel lens, 12x optical zoom) to confirm DR development. A portable ERG mini-Ganzfield (HMsERG RetVet) unit was used at different disease development stages: non-diabetic, diabetic, and after hNPCs therapy. A high-intensity ERG (average of four flashes, 0.5 Hz, 1 log CDs/m^2) was performed under scotopic conditions (12 h dark adaptation).

2.3.3. Optical coherence tomography

OCTy (Spectralis OCT, Heidelberg Engineering) assessed the retinal layer morphology in pre and posted hNPCs therapy animals. Before the exam, pupils were dilated using 1% tropicamide, and animals were anesthetized by ip injection using a combination of ketamine (60 mg/kg) / xylazine (10 mg/kg). Two retinal thickness measurements were made in two horizontal sections (above and below optic nerve) of both eyes in each animal.

2.4. hNPCs marking

The cells were incubated with Qtracker® 655 Cell Labeling Kit (Thermo Fisher®) on the transplant day, as recommended. The nanocrystals provide a red stable fluorescence into the cell cytoplasm (manufacturer statement).

2.4.1. Intravitreal administration of hNPCs

Freshly trypsinized passage four hNPCs (1 x 10^6 cells/µL), suspended in 5 µL of physiological solution, were used for transplantation at eight weeks post-injection STZ and confirmed DR installation. The rats were anesthetized with combined ketamine and xylazine via ip. The pupils were dilated, and a corneal anesthetic was applied (Anestalcon®, Alcon).

The rats from the DM+hNPCs group received a single intravitreal injection on each eye, slowly injected in the vitreous cavity through *pars plana*. Hylo© Gel (Ursapharm) was applied to the eyes after intravitreal injections [27]. For all injections, an insulin needle was used.

2.4.2. hNPCs tracking

The hNPCs with Qtracker® 655 were tracked four weeks post-transplant, after animal euthanasia and eye enucleation, to observe cell migration, distribution, and integration into retinal layers. Retinal sections were prepared with frozen optimal cutting temperature compound in cryostat equipment (5µm) and stored at -20 °C.

The sections were washed with PBS until the compound was removed, a drop of SlowFade™ Gold Antifade Mountant with DAPI (Thermo Fisher®) nuclei staining was applied, covered with a coverslip, and the slides were sealed. Images were taken using fluorescent optical microscopy (Zeiss Axio Scope A1 microscopy).

 doi:10.20944/preprints202106.0268.v1

2.5 Histopathology and Immunohistochemistry (IHC) techniques

Histopathology was performed four weeks post-treatment. The animals were anesthetized, euthanized, and eyes enucleated. Eyes were fixed in 4% formalin, paraffin-embedded, and histological sections were stained with hematoxylin and eosin (H&E). Proteins of interest, such as glial fibrillary acid protein (GFAP), vascular endothelial growth factor receptor 1(VEGFR 1), neuron-glial antigen-2 (NG-2), and rhodopsin, were identified by IHC using antibodies anti-GFAP (monoclonal, clone 6F2, mouse, Dako, M0761, 1:200), anti-VEGFR 1 (polyclonal, rabbit, Thermo Fisher® PA1-21731, 1:50), anti-NG2 (polyclonal, rabbit, Abcam, ab129051, 1:200), and anti-Rhodopsin (polyclonal, rabbit, Sigma Aldrich®, SAB4502636, 1:100).

The secondary antibody was Reveal Polyvalent HRP-DAB Detection System, Spring Bioscience®. Specificity controls were performed by (i) omitting the primary antibody (negative control) and (ii) testing retina samples of rats (positive controls).

2.5.1 IHC Morphometric analysis

After IHC staining, the slide scanner Axio Scan.Z1 (Zeiss) digitalized the paraffin-embedded slides, generating files with the czi extension, through the software ZEN 3.1 blue edition (Zeiss). The files were visualized, and each file (slide) generated numerous images in 200 x magnification fields. The images were submitted to Adobe Photoshop C6 (Adobe) to exclude structures of no interest. The morphometry software Image-Pro plus 4.5 (Media Cybernetics) was used to quantify the areas of immunopositivity. The semi-automatic color segmentation method was used so that each color hue of the reaction (brown for immunopositive areas and blue for areas without immunoexpression) was manually selected based on qualitative visual observation and saved as a file. The resulting file, named mask, had the function of standardizing the immunoexpression intensity color. The mask was then applied to each of the images, used to quantify the areas of the respective antibodies.

The values of immunoreaction intensity concerning the total tissue area were exported to an Excel spreadsheet and submitted to statistical analysis.

3. Statistical analysis of IHC

For comparison of the groups, the non-parametric Kruskal-Wallis test was used. Multiple posthoc comparisons were made using Dunn's test. Values of $p<0.05$ indicated statistical significance. The data were analyzed with the GraphPad Prism version 5.

4. Results

4.1. Flow cytometry analysis of WJ-MSCs

Flow cytometry analysis of WJ-MSCs revealed the positivity (CD90, CD105, CD73, HLA-ABC), negativity (CD34, CD45, HLA-DR), and cell viability (Figure 1).

Preprints (www.preprints.org) | NOT PEER-REVIEWED | Posted: 9 June 2021 doi:10.20944/preprints202106.0268.v1

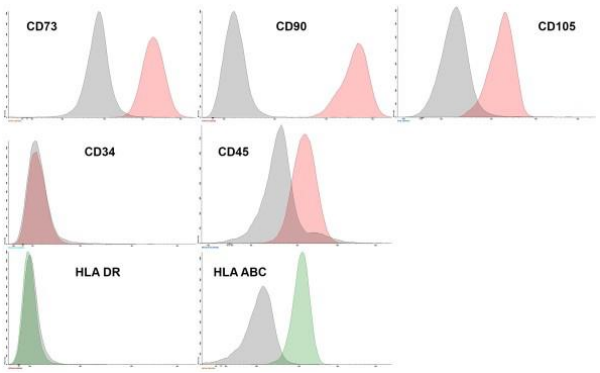

Figure 1. Representative flow cytometry histogram of WJ-MSCs sample. The red peak represents positivity for antibodies: CD90, CD105, CD73 and negativity for antibodies: CD34, CD45; in green, the negativity for the HLA-DR antibody and positivity for the HLA-ABC; and in gray, the isotypic control demarcating the area in which the samples are negative for a specific marker. The samples were analyzed in biological triplicates and represented in percentage. CD73+, CD90+, CD105+, CD34-, CD45- (99,50%), HLA-DR- (100%) and HLA-ABC+ (99,13%). The result of cell viability was 93.13%. Abbreviation: WJ-MSCs, Wharton's jelly - mesenchymal stem cells.

4.2. Immunocytochemistry

The presence of neural precursor cell elements was confirmed by anti-nestin and anti-β-III tubulin antibodies analyses (Figure 2).

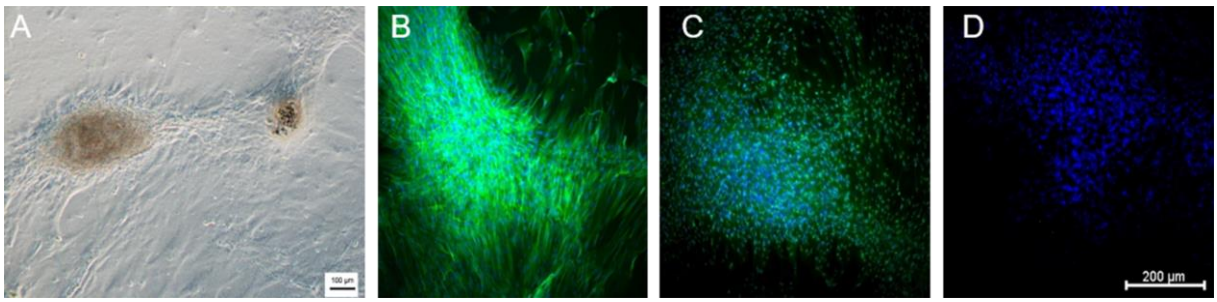

Figure 2. (A) Neurosphere development, inverted optical microscopy. Scale bar, 100 μm; (B) hNPCs from neurospheres labeled with anti-nestin FITC antibody and Hoechst, (C) hNPCs from neurospheres labeled with anti- β -III tubulin FITC antibody and Hoechst, (D) Nuclei stained with Hoechst. Images: (B-D) IN Cell Analyzer 2000 Imaging System, GE Healthcare, UK equipment. Scale bar, (B-D) 200 µm.

4.3. Diabetes and DR evaluation

4.3.1. Hyperglycemia

Hyperglycemia identified diabetic rats. After STZ-induction of type I diabetes, an increase in glucose levels was observed and remained throughout the study, demonstrated by means ± SD, at times: before induction, after ten days, and after 30 days of induction (blood glucose levels 106.44 ±5.66 mg/dL; 333.50 ±106.72 mg/dL, and 452.72 ±74.65

Preprints (www.preprints.org) | NOT PEER-REVIEWED | Posted: 9 June 2021 doi:10.20944/preprints202106.0268.v1

mg/dL, respectively). The development of cataracts was observed in 31 percent of induced rats after 6 to 8 weeks, as an earlier complication of DM progression. No massive eye hemorrhage was observed after cell solution injection.

4.3.2 Topical Endoscopy Fundus Imaging (TEFI)

In vivo TEFI exams were performed to verify signals that were compatible with DR (Figure 3). The differences between ND vs. DM rats certified that DR was installed, though some characteristics.

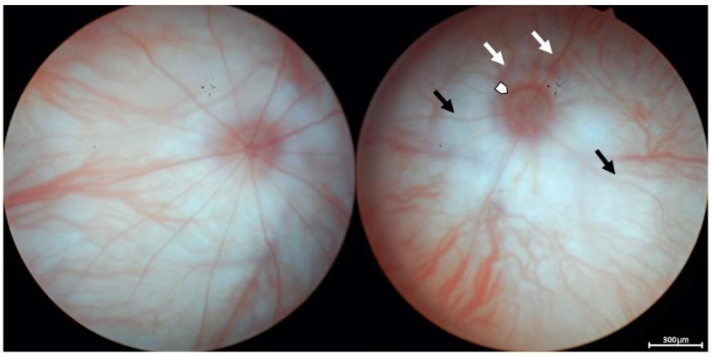

Figure 3. Representative fundus images. (A) ND (right eye); (B) DM (right eye). Note that the larger retinal blood vessels started to dilate (white arrow) and became irregular (black arrows). In the edematous area, the nerve fiber layer generalized fuzzy appearance in the central retina and areas adjacent to the optic disc. Note the neovascularization of the optic disc (white arrowhead). Abbreviation: ND, non-diabetic rat; DM, diabetic rat. Scale bar, 300µm.

4.3.3. Electroretinography (ERG)

The oscillatory potentials (OPs) of the ERG results were significantly higher post-treatment (*p=0.02), analyzed by ERGView (Ocuscience, Nevada, USA). The mean amplitude of the OPs pre-treatment was 110.32 ± 9.07 µV and post-treatment 267.50 ± 78.89 µV (Figure 4). There were no significant differences pre vs. post- ERG a- and b-wave amplitudes and implicit times. A-wave amplitudes were pre 208.4 ± 15.56 µV and post 211.7 ± 28.31 µV. A-wave implicit time was pre 18.50 ± 12.51 ms, post 19.20 ± 8.66 ms; B-wave amplitude pre 545.50 ± 64.77 µV, post 490.66 ± 64.39 µV. B-wave implicit time was 47.70 ± 9.34 ms, post 61.43 ± 27.90 ms.

Preprints (www.preprints.org) | NOT PEER-REVIEWED | Posted: 9 June 2021 doi:10.20944/preprints202106.0268.v1

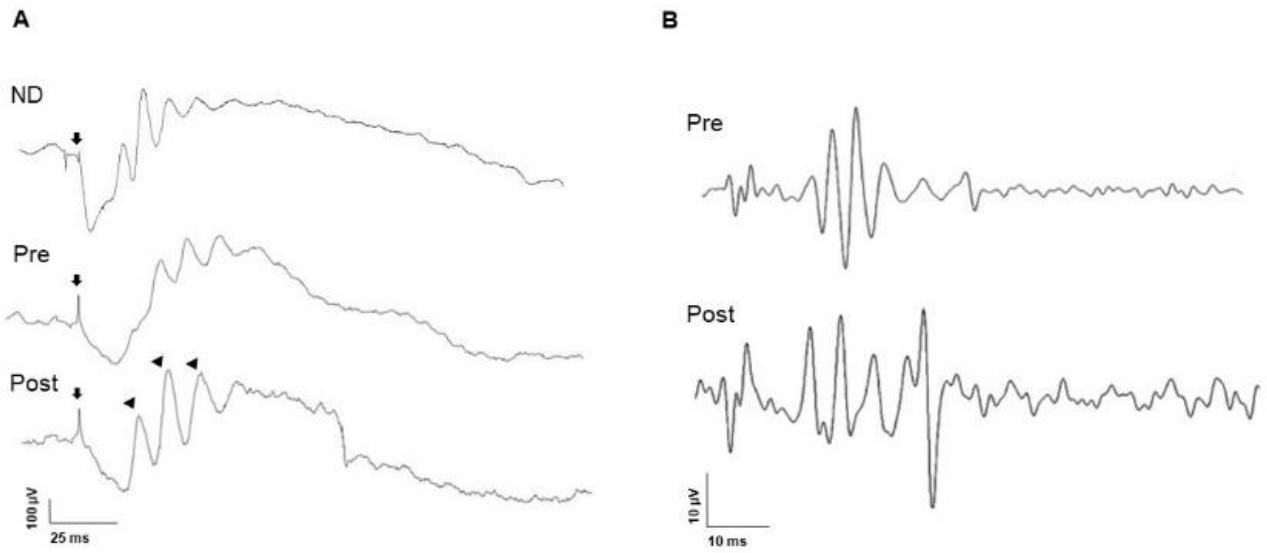

Figure 4. Representative electroretinography (ERG) results. (A) ERG tracings groups: ND; pre, and post-treatment with hNPCs in a rat with DM. Note that the a-and b-wave amplitudes, as well as implicit times, are equivalent. The amplitudes of the OPs were significantly higher post-treatment (arrowheads); arrows indicate stimulus onset. (B) The mean amplitude of the OPs pre-treatment was 110.32 ± 9.07 µV and post-treatment 267.50 ± 78.89 µV. OPs extraction - ERGView (Ocuscience, Nevada, USA). Abbreviations: ERG, electroretinography; ND, non-diabetic; hNPCs, human neural precursor cells; Ops, oscillatory potential.

4.3.4. Optical Coherence Tomography (OCT)

Intravitreal injection of hNPCs reversed apoptosis of retinal neural layers. At OCT, two measurements of retinal thickness were made in two horizontal sections (above and below optic nerve head) of each animal, and results were analyzed using Graphpad Prism software ($p < 0.05$). Statistical comparison between groups was performed using *t-test* (p - Give 95% confidence intervals for main findings (Figure 5). DM and DM+hNPCs rats were used to analyze retinal layers and their thickness in the pre and post-transplant times.

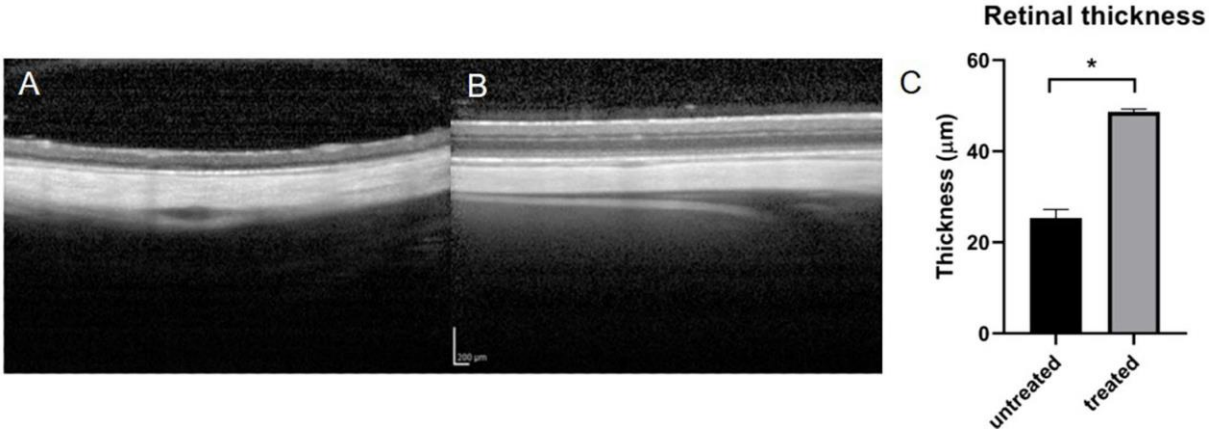

Figure 5. Sections of optical coherence tomography (OCT) of diabetic rats before and after treatment. (A) Diabetic rat without cell treatment shows a decrease in the thickness of the retina layers and signs of apoptosis in some layers; (B)

Preprints (www.preprints.org) | NOT PEER-REVIEWED | Posted: 9 June 2021 doi:10.20944/preprints202106.0268.v1

Rat treated with hNPCs presented improvement in retinal thickness and all retina layers; (C) Graphic representation of the retinal thickness in untreated and treated animals: scale bar, 200μm.

4.4. hNPCs tracking

Intravitreal transplanted cells were tracked by fluorescence techniques (Figure 6). hNPCs migration across the entire retinal length and integration into the Retinal Pigment Epithelium (RPE) were noticed.

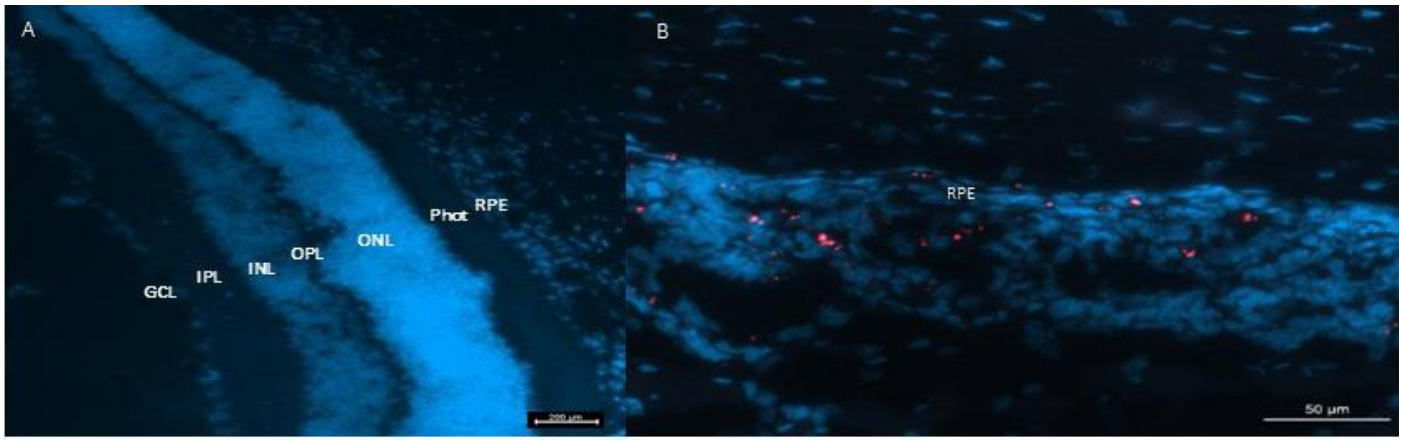

Figure 6. Retinal cryostat sections (5μm). The microscopy slides were DAPI stained to visualize nuclei, using optical fluorescence microscopy; (A) Images showing the layers of the neuronal retina, ND rat; (B) High-magnification confocal microscopy image showing combined DAPI (blue), and Qtracker® (red) into hNPCs, four weeks post-transplant, evidencing hNPCs migration and integration to RPE. DAPI image ex (425-475nm), Qdot® ex (663-738nm). Abbreviations: DAPI, (4'6-diamidino-2-phenylindole); ND, non-diabetic rat; hNPCs, human neural precursor cells; cell layer; IPL, inner plexiform layer; INL, inner nuclear layer; OPL, outer plexiform layer; ONL, outer nuclear layer; Phot, photoreceptors; RPE, retinal pigment epithelium. Scale bars, (A) 200μm; (B, C) 50μm.

4.5. Histopathological and IHC results

Histopathological sections (H&E) of rat retina demonstrated morphological changes in DR and after cell treatment (Figure 7A-C). The morphological retina structures presented regular arrangement at ND. Compatible alterations with DR were evidenced by several changes, including the loss of retinal ganglion cells at DM. There was an effective enhancement of all layers in the treated group. Immunohistochemistry for GFAP (7D-F) verified the distribution of GFAP at GCL as a specific marker to astrocytes. VEGF (7G-I) associated with the early breaking of the BRB and stimulation of angiogenesis was evident in the DR. The hNPCs led to a decrease of VEGF secretion, similar to the ND group. The pigment Rhodopsin (7J-L) localized in the rods of photoreceptors showed loss of the RPE and rods in DR and structural disorder. There was an increase of photoreceptors layer thickness and Rhodopsin marking in the treated group. NG2 (7M-O) expressed by pericytes demonstrated the microvascular complications induced by hyperglycemia in DR, leading to apoptosis. Higher NG2 expression in a treated group is associated with vasculature stabilization.

Preprints (www.preprints.org) | NOT PEER-REVIEWED | Posted: 9 June 2021 doi:10.20944/preprints202106.0268.v1

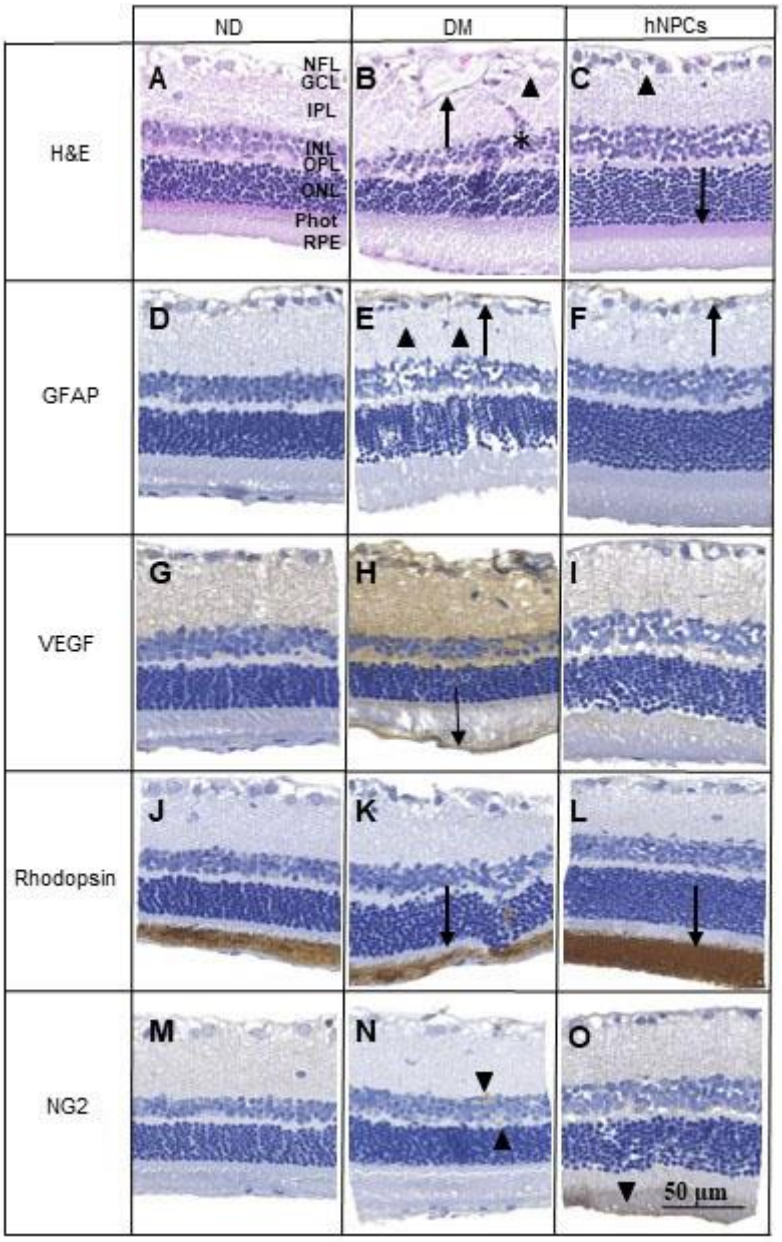

Figure 7. Haematoxylin & Eosin (H&E) stained sections of the retina. (A-C) (A) ND, Morphological retina structures with the regular arrangement; (B) DM, the retinal layers are irregular and disorganized, marked loss and disruption of GCL (arrowhead), abnormal microvasculature (*), vacuolar degeneration (arrow), and damage to the Phot; (C) treated hNPCs group, a significant increase and arranged GCL (arrowhead), improvement of all retinal layers, enhanced of Phot (↑). Immunohistochemistry (IHC) reactive for antibodies (D-F) GFAP; (D) ND, marker limited to astrocytes at GCL and NFL; (E) GCL and NFL degeneration, apoptosis with an increase at GFAP level (↑), projections from GCL into IPL (arrowhead), also pronounced disruption in the other layers; (F) hNPCs ameliorate compromised layers, reduced projections into IPL, evidenced improvement at GCL and NFL (↑); (G-I) VEGF; (G) normal immunoreactivity; (H) Vascular lesions and BRB (↑) breakdown demonstrated by the damage on the microenvironment of the retina with VEGF immunoreactivity; (I) The treatment indicated a decrease at VEGF secretion, contributing to the integrity of the BRB; (J-L) Rhodopsin; (J) Rhodopsin marking of rods; (K) Disruption and loss of photoreceptors (↑); (L) hNPCs treated group had an increase of photoreceptors and RPE layers (↑); (M-O) NG2; (M) regular NG2 immunoreaction; (N) Pericytes evidenced in the inner retinal capillaries (arrowhead) at microvascular abnormalities; (O) hNPCs treatment evidenced the ability to protect retinal capillaries, to support the maintenance of retinal microvessel, including the BRB (arrowhead). Abbreviations: ND, non-diabetic; DM, diabetic; hNPCs, human neural precursor cells; GCL, ganglion cell layer; Phot, photoreceptors; NFL, nerve fiber layer; GFAP,

Preprints (www.preprints.org) | NOT PEER-REVIEWED | Posted: 9 June 2021 doi:10.20944/preprints202106.0268.v1

glial fibrillary acidic protein; IPL, inner plexiform layer; VEGF, vascular endothelial growth factor; BRB, retinal blood barrier; NG2, neural/glial antigen 2; INL, inner nuclear layer; OPL, outer plexiform layer; ONL, outer nuclear layer; RPE, retinal pigment epithelium. Scale bar, 50μm.

4.6. Statistical analysis of IHC

The quantitative data analysis (Table 1) from the immunohistochemistry observations of protein markers revealed differences comparing the three groups (Figure 8). Data were analyzed by GraphPad Prism 5, non-parametric Kruskal-Wallis test, and posthoc Dunn's test, four weeks post-treatment. The results showed no significant difference between groups for the GFAP and VEGF. There were significant differences in the level of Rhodopsin protein between ND and hNPCs; the level of NG2 protein between ND and hNPCs, and between DM and hNPCs.

Table 1. Proteins markers quantitative data correspondent to mean ± SD, four weeks after treatment.

Marker	Group	Mean ± SD
GFAP	ND	0.8547 ± 0.7658
	DM	0.6199 ± 0.3683
	hNPCs	1.153 ± 0.8057
VEGF	ND	4.943 ± 3.833
	DM	13.38 ± 11.69
	hNPCs	5.021 ± 5.110
RHODOPSIN	ND	7.790 ± 5.116
	DM	11.88 ± 2.521
	hNPCs	14.96 ± 2.916
NG2	ND	0.5728 ± 0.2963
	DM	1.187 ± 0.7292
	hNPCs	3.966 ± 2.294

Abbreviations: SD, standard deviation; GFAP, glial fibrillary acidic protein; VEGF, vascular endothelium growth factor; NG2, neural/glial antigen 2; ND, non-diabetic; DM, diabetic; hNPCs, human neural precursor cells.

Preprints (www.preprints.org) | NOT PEER-REVIEWED | Posted: 9 June 2021 doi:10.20944/preprints202106.0268.v1

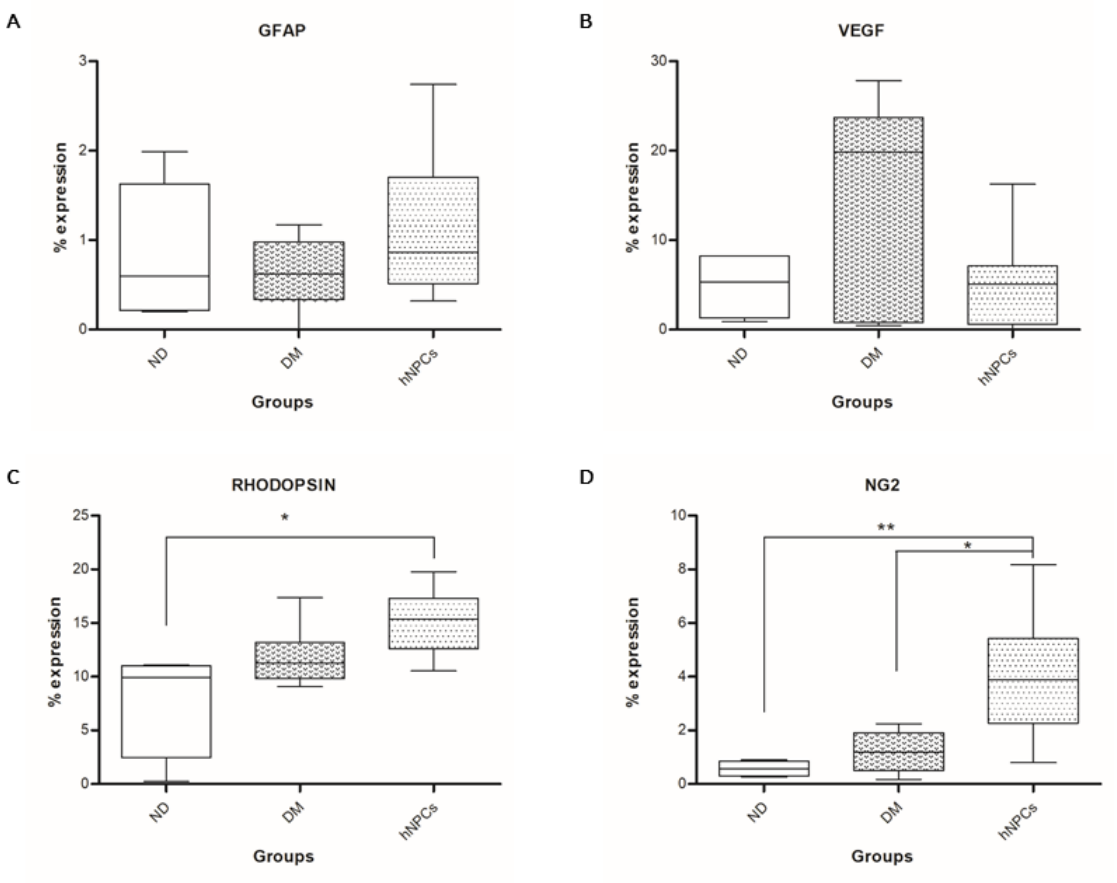

Figure 8. Representative immunohistochemistry protein expression presented in percentage (Mean ± SD), without significant difference between groups for the (A) GFAP and (B) VEGF. There were significant differences for (C) Rhodopsin protein ND vs. hNPCs **p=0.0074; (D) NG2 protein ND vs. hNPCs **p=0.0015, DM vs. hNPCs *p<0.05). Abbreviations: ND, non-diabetic group; DM, diabetic group; hNPCs, human neural progenitor cells group; GFAP, glial fibrillary acid protein; VEGF, vascular endothelial growth factor; NG2, neural/glial antigen 2.

5. Discussion

Patients with DR have a low quality of life, considering gradual visual decline and blindness. DR has no cure, and all types of treatments and drugs developed only delay its progression [1]. Therefore, advances in the understanding of pathophysiology pave the way for promising discoveries. The umbilical cord is a biological material with many advantages. It is a hospital disposal material, with minor ethical concerns attributed to the cells isolated from it, requiring only a signed written informed consent form for a non-invasive tissue collection. WJ-MSCs are a promising tool in cellular therapy for regenerative medicine and immunotherapy [28]. Cell transplantation has been used in preclinical studies to treat several diseases, including ophthalmological ones [17, 29].

A significant enhancement has been observed in diabetic rats post-treatment with hNPCs derived from WJ-MSCs, through improved visual function, recuperation of retinal cell layer morphology, and better response to specific antibodies. The most relevant differences in morphological analysis of treated animals compared to untreated ones, with the improvement of the retina, were observed in the GCL, BRB, RPE, and Photoreceptor layers. The WJ-MSCs differentiation into the NPC state, without growth factors, is a promising strategy for stem cell therapy, with possibly fewer adverse effects from the additives. Similar results were obtained in a previous study with neural

Preprints (www.preprints.org) | NOT PEER-REVIEWED | Posted: 9 June 2021 doi:10.20944/preprints202106.0268.v1

stem cells from WJ-MSCs [29], proposing that WJ-MSCs are an alternative for the treatment of DR after MSCs differentiation to NPCs with a neurobasal media growth factor [29].

Four weeks post-transplant WJ-MSCs presented a neuroprotection effect in a crushed optic nerve rat model, promoting the integration, and delaying the loss of retinal ganglion cells [17]. The combinations of neuroprotective and immunomodulatory capacities of WJ-MSCs and hNPCs cell therapies may provide the therapeutic potential recommended for pathological changes in retinal ganglion cells [30].

At ERG recordings, the efficiency of hNPCs treatment was verified through the difference in the oscillatory potentials (OPs) amplitudes at pre, and post-transplant, suggesting the recuperation of visual function. The significantly higher OPs post-treatment is relevant since the drop in the values predicts the progression to a severe proliferative diabetic retinopathy stage in patients [12]. The recuperated retinal thickness post-transplant observed by OCT and ERG results demonstrated the therapeutic effect of the hNPCs treatments for DR [31,32].

In response to the inflammatory process of DR in early experimental diabetes, astrocytes and Müller cells act as neuroprotectors increasing GFAP expression [33]. Whereas glial cells stimulate barrier properties and tight junction protein expression, cell alterations and death as the disease progresses lower the capacity to maintain the BRB integrity and decrease the expression of GFAP [34]. Differences in GFAP immunoreactivity were not significant, besides the pronounced disruption in the NFL and GCL in *diabetes* and repair of these layers after hNPCs treatment.

VEGF has a protective capacity at normal levels for neuronal survival and is produced in many retinal cell types [35]. The VEGF expression and release can be an adaptive response of the oxidative stress in pathological conditions like DR, and its increase is associated with vascular permeability and neovessels, leading to retinal dysfunction [34, 35]. Herein, the hNPCs treatment must have acted in the regulation for VEGF secretion, normalizing vascular permeability, supporting GCL and Müller cells, reducing its pathological angiogenic state, preventing neovascularization or hypoxia. In this context, the mechanisms that hNPCs used to protect neurons could also be explained by inhibiting oxidative stress and decreasing VEGF overexpression [36].

The rhodopsin, a photosensitive protein, is localized in the rods of photoreceptors [37]. The structural disorder of photoreceptors was evident in the DM group, contrary to the hNPCS treated group. Regular organization of the photoreceptor layer as evidenced by the expression of rhodopsin, with the potential a biomarker for monitoring neurodegenerative diseases, including in the retina [38].

The RPE is a primordial layer in the visual process as part of many steps of the proper development and function of the retina, such as transepithelial transport, phagocytosis, and light absorption [39], with close interaction with the blood-retinal barrier (BRB). The intravitreal administrated hNPCs migrated across the entire retinal length, integrated into the RPE, improved and rearranged the structures of the retina. The route that triggered the repair by the hNPCs and factors supported by them should be more investigated. Cell transplantation from fetal RPE, MSCs, or their combination has demonstrated the advantages of combined cells in the rodent retinal degeneration model [31].

NG2 is expressed by pericytes in response to microvascular complications induced by hyperglycemia, leading to apoptosis, and its loss is irreversible in DR [40]. However, the replenishment of pericytes and perivascular progenitor cells could restore vascular integrity, preventing fluid leakage [40]. The hNPCs treatment promoted a significant increase of pericytes, possibly protecting the retinal capillaries, supporting the maintenance of retinal microvessels and the BRB.

This study presents different hypotheses for the beneficial results observed with hNPCs intravitreal cell therapy. Considering DR a microvascular and neurodegenerative disease [4], with compromised signaling between glial cells and blood vessels [41], hNPCs demonstrated a contribution to repair the integrity of the BRB, as observed in the IHC for NG2 (a proteoglycan) linked to pericytes at vascular morphogenesis.

 doi:10.20944/preprints202106.0268.v1

Pericytes mediated the capillary diameter in conjunction with endothelial cells, combining neural activity with increased capillary blood flow [42, 43, 44], Suggesting the regulation effect on blood flow, reflecting in the recovery of neural activity control. Also, pericytes present MSC markers, trilineage differentiation, and contribute to the activation of endogenous stem cells [45, 46], participate in various physiological functions, and are recruited in various situations. Under certain culture conditions, pericytes may form neuronal progenitors [47]. These shreds of evidence propose that hNPCs may have the ability to stimulate retinal pericytes, supporting microcirculation, bringing relief from vascular symptoms by participating in the natural repair process, and hNPCs may have generated ideal conditions to form neuronal progenitors.

hWJMSCs paracrine effect, with the secretion of anti-inflammatory molecules and trophic factors, evoked the neuroprotection, as the characteristics of the niche where the cells are transplanted to or migrated to can modulate their secretome [17]. As described previously, NPCs are an undifferentiated lineage of neural stem cells, including progenitor cells and neural stem cells [19]. The hNPC cell population may have the required factors for mediating effectiveness improvements in the neuroretinal environment, as observed in studies that reported better results for tissue regeneration using combined cell transplantation treatment compared to a single cell type treatment [48, 31].

Several different types of stem cells are being explored [49], herein is pointed that for the neuronal environment of the retina, cells of the same ancestry can be the ones that bring a more significant benefit in the repair of DR.

hNPCs could have resulted in the retinal repair by their differentiation, being niche dependent as the cells were crossing the affected layers, or as a stimulator for the retinal progenitor cells, interacting with the endogenous regenerative cycle, both conditions with the promisor potential functional rescue of DR.

6. Conclusions

In conclusion, these findings demonstrate the capacity of hNPCs for migration, integration, and repair of tissue cytoarchitecture of the retina to promote retinal neuroregeneration by paracrine effects in diabetic retinopathy. The cell therapy with intravitreal transplanted hNPCs was effective, suggesting that it could be considered in the treatment of DR and other blinding retinal disorders.

Supplementary Materials: The following are available online at www.mdpi.com/xxx/s1, Figure S1: title, Table S1: title, Video S1: title.

Author Contributions: **Author Contributions**: Conceptualization, C.S.S and K.A.T.C.; Methodology, C.S.S, P.E.F.S, B.F.M, A.C.I, J.M, C.R.C.F and S.N.; validation, C.S.S and K.A.T.C.; formal analysis, C.S.S, K.A.T.C.; investigation, C.S.S, B.F.M, M.C.P, F.M-F, P.D, M.S, N.S and L.N.; statistical analysis, C.S.S and B.F.M; resources, K.A.T.C.; data curation, C.S.S and K.A.T.C.; writing—original draft preparation, C.S.S, K.A.T.C, M.B-G and E.A.; writing—review and editing, C.S.S, K.A.T.C and D.S.M.D.; supervision, K.A.T.C.; project administration, K.A.T.C.; funding acquisition, K.A.T.C. All authors have read and agreed to the published version of the manuscript.

Funding: This research received no external funding. First author was MSc student of Pequeno Príncipe Faculties with Grant from Coordination for the Improvement of Higher Education Personnel- Brazil (CAPES).

Institutional Review Board Statement: According to the guidelines of the Declaration of Helsinki, the study was conducted and approved by the Research Ethics Human Committee of Pequeno Príncipe Faculties authorization, Approval number 3.288.297 – Date April-26th-2017 at the Hospital Maternidade Victor Ferreira do Amaral (Curitiba, Brazil).

 doi:10.20944/preprints202106.0268.v1

Informed Consent Statement: Informed consent was obtained from all subjects involved in this study, the donors of Umbilical Cord.

Data Availability Statement: Not applicable.

Acknowledgments: We thank Coordination for the Improvement of Higher Education Personnel- Brazil (CAPES), Finance code 001.

Conflicts of Interest: The authors declare that they have no conflict of interest.

References

(1) Fong, D. S.; Aiello, L. P.; Ferris, F. L.; Klein, R. Diabetic Retinopathy. *Diabetes Care* **2004**, *27* (10), 2540. https://doi.org/10.2337/diacare.27.10.2540.

(2) *Global Report on Diabetes*; Roglic, G., World Health Organization, Eds.; World Health Organization: Geneva, Switzerland, 2016.

(3) Antonetti, D. A.; Barber, A. J.; Bronson, S. K.; Freeman, W. M.; Gardner, T. W.; Jefferson, L. S.; Kester, M.; Kimball, S. R.; Krady, J. K.; LaNoue, K. F.; Norbury, C. C.; Quinn, P. G.; Sandirasegarane, L.; Simpson, I. A. Diabetic Retinopathy: Seeing Beyond Glucose-Induced Microvascular Disease. *Diabetes* **2006**, *55* (9), 2401–2411. https://doi.org/10.2337/db05-1635.

(4) Barber, A. J.; Baccouche, B. Neurodegeneration in Diabetic Retinopathy: Potential for Novel Therapies. *Vision Res.* **2017**, *139*, 82–92. https://doi.org/10.1016/j.visres.2017.06.014.

(5) Stem, M. S.; Gardner, T. W. Neurodegeneration in the Pathogenesis of Diabetic Retinopathy: Molecular Mechanisms and Therapeutic Implications. *Curr. Med. Chem.* **2013**, *20* (26), 3241.

(6) Sohn, E. H.; van Dijk, H. W.; Jiao, C.; Kok, P. H. B.; Jeong, W.; Demirkaya, N.; Garmager, A.; Wit, F.; Kucukevcilioglu, M.; van Velthoven, M. E. J.; DeVries, J. H.; Mullins, R. F.; Kuehn, M. H.; Schlingemann, R. O.; Sonka, M.; Verbraak, F. D.; Abràmoff, M. D. Retinal Neurodegeneration May Precede Microvascular Changes Characteristic of Diabetic Retinopathy in Diabetes Mellitus. *Proc. Natl. Acad. Sci.* **2016**, *113* (19), E2655–E2664. https://doi.org/10.1073/pnas.1522014113.

(7) B. Arden, G.; Sivaprasad, S. Hypoxia and Oxidative Stress in the Causation of Diabetic Retinopathy. *Curr. Diabetes Rev.* **2011**, *7* (5), 291–304. https://doi.org/10.2174/157339911797415620.

(8) Brownlee, M. The Pathobiology of Diabetic Complications. *Diabetes* **2005**, *54* (6), 1615. https://doi.org/10.2337/diabetes.54.6.1615.

(9) Shimizu, K.; Kobayashi, Y.; Muraoka, K. Midperipheral Fundus Involvement in Diabetic Retinopathy. *Ophthalmology* **1981**, *88* (7), 601–612. https://doi.org/10.1016/S0161-6420(81)34983-5.

(10) de Hoz, R.; Rojas, B.; Ramírez, A. I.; Salazar, J. J.; Gallego, B. I.; Triviño, A.; Ramírez, J. M. Retinal Macroglial Responses in Health and Disease. *BioMed Res. Int.* **2016**, *2016*, 1–13. https://doi.org/10.1155/2016/2954721.

(11) Rübsam, A.; Parikh, S.; Fort, P. Role of Inflammation in Diabetic Retinopathy. *Int. J. Mol. Sci.* **2018**, *19* (4), 942. https://doi.org/10.3390/ijms19040942.

(12) Bresnick, G. H.; Palta, M. Predicting Progression to Severe Proliferative Diabetic Retinopathy. *Arch. Ophthalmol.* **1987**, *105* (6), 810–814. https://doi.org/10.1001/archopht.1987.01060060096041.

(13) Frizziero, L.; Midena, G.; Longhin, E.; Berton, M.; Torresin, T.; Parrozzani, R.; Pilotto, E. Early Retinal Changes by OCT Angiography and Multifocal Electroretinography in Diabetes. *J. Clin. Med.* **2020**, *9* (11), 3514. https://doi.org/10.3390/jcm9113514.

(14) Hsieh, J.-Y.; Wang, H.-W.; Chang, S.-J.; Liao, K.-H.; Lee, I.-H.; Lin, W.-S.; Wu, C.-H.; Lin, W.-Y.; Cheng, S.-M. Mesenchymal Stem Cells from Human Umbilical Cord Express Preferentially Secreted Factors Related to Neuroprotection, Neurogenesis, and Angiogenesis. *PLoS ONE* **2013**, *8* (8), e72604. https://doi.org/10.1371/journal.pone.0072604.

(15) Ke, M.; Ml, W.; Bm, M.; P, M.; D, D.; L, M.; B, H.; M, B.; K, A.-E.; T, H.; D, T.; S, M. Matrix cells from Wharton's jelly form neurons and glia https://pubmed.ncbi.nlm.nih.gov/12529551/ (accessed Jan 4, 2021). https://doi.org/10.1634/stemcells.21-1-50.

(16) Reynolds, B. A.; Weiss, S. Clonal and Population Analyses Demonstrate That an EGF-Responsive Mammalian Embryonic CNS Precursor Is a Stem Cell. *Dev. Biol.* **1996**, *175* (1), 1–13. https://doi.org/10.1006/dbio.1996.0090.

(17) Millán-Rivero, J. E.; Nadal-Nicolás, F. M.; García-Bernal, D.; Sobrado-Calvo, P.; Blanquer, M.; Moraleda, J. M.; Vidal-Sanz, M.; Agudo-Barriuso, M. Human Wharton's Jelly Mesenchymal Stem Cells Protect Axotomized Rat Retinal Ganglion Cells via Secretion of Anti-Inflammatory and Neurotrophic Factors. *Sci. Rep.* **2018**, *8* (1), 16299. https://doi.org/10.1038/s41598-018-34527-z.

(18) Differentiation of Isolated Human Umbilical Cord Mesenchymal Stem Cells into Neural Stem Cells. *Int. J. Ophthalmol.* **2016**, *9* (1). https://doi.org/10.18240/ijo.2016.01.07.

(19) Mini-Review: Neural Stem Cells https://www.stemcell.com/neural-stem-cells-lp.html (accessed Jan 4, 2021).

(20) The ARRIVE guidelines 2.0: Updated guidelines for reporting animal research https://journals.plos.org/plosbiology/article?id=10.1371/journal.pbio.3000410 (accessed Jan 4, 2021).

(21) Cho, H.; Seo, Y.-K.; Jeon, S.; Yoon, H.-H.; Choi, Y.-K.; Park, J.-K. Neural Differentiation of Umbilical Cord Mesenchymal Stem Cells by Sub-Sonic Vibration. *Life Sci.* **2012**, *90* (15–16), 591–599. https://doi.org/10.1016/j.lfs.2012.02.014.

(22) Dominici, M.; Le Blanc, K.; Mueller, I.; Slaper-Cortenbach, I.; Marini, F. C.; Krause, D. S.; Deans, R. J.; Keating, A.; Prockop, D. J.; Horwitz, E. M. Minimal Criteria for Defining Multipotent Mesenchymal Stromal Cells. The International Society for Cellular Therapy Position Statement. *Cytotherapy* **2006**, *8* (4), 315–317. https://doi.org/10.1080/14653240600855905.

(23) Irioda, A. C.; Cassilha, R.; Zocche, L.; Francisco, J. C.; Cunha, R. C.; Ferreira, P. E.; Guarita-Souza, L. C.; Ferreira, R. J.; Mogharbel, B. F.; Garikipati, V. N. S.; Souza, D.; Beltrame, M. P.; de Carvalho, K. A. T. Human Adipose-Derived Mesenchymal Stem Cells Cryopreservation and Thawing Decrease α 4-Integrin Expression. *Stem Cells Int.* **2016**, *2016*, 1–9. https://doi.org/10.1155/2016/2562718.

(24) Carvalho, K.; Stricker, P. E. F.; Souza, D. de; Irioda, A. C.; Mogharbel, B. F.; Franco, C. R. C.; Leitec, J. R. de S. A.; jo, A. R. de A.; Borgese, F. A.; Herculano, R. D.; Graefff, F. de O. *DIFFERENTIATION OF HUMAN MESENCHYMAL STEM CELLS THROUGH THE NATURAL MATRIX TO NEUROSPHERES FOR CHOLINERGIC-LIKE CELLS*; preprint; Preprints, 2020. https://doi.org/10.22541/au.159620987.78611470.

(25) Trzaska, K. A.; Rameshwar, P. Dopaminergic Neuronal Differentiation Protocol for Human Mesenchymal Stem Cells. In *Mesenchymal Stem Cell Assays and Applications*; Vemuri, M., Chase, L. G., Rao, M. S., Eds.; Methods in Molecular Biology; Humana Press: Totowa, NJ, 2011; Vol. 698, pp 295–303. https://doi.org/10.1007/978-1-60761-999-4_22.

(26) Guidelines on Use of Streptozotocin in Rodents | Research A to Z https://az.research.umich.edu/animalcare/guidelines/guidelines-use-streptozotocin-rodents (accessed Jan 4, 2021).

(27) Ezquer, M.; Urzua, C. A.; Montecino, S.; Leal, K.; Conget, P.; Ezquer, F. Intravitreal Administration of Multipotent Mesenchymal Stromal Cells Triggers a Cytoprotective Microenvironment in the Retina of Diabetic Mice. *Stem Cell Res. Ther.* **2016**, *7* (1), 42. https://doi.org/10.1186/s13287-016-0299-y.

(28) Nagamura-Inoue, T. Umbilical Cord-Derived Mesenchymal Stem Cells: Their Advantages and Potential Clinical Utility. *World J. Stem Cells* **2014**, *6* (2), 195. https://doi.org/10.4252/wjsc.v6.i2.195.

(29) Zhang, W.; Wang, Y.; Kong, J.; Dong, M.; Duan, H.; Chen, S. Therapeutic Efficacy of Neural Stem Cells Originating from Umbilical Cord-Derived Mesenchymal Stem Cells in Diabetic Retinopathy. *Sci. Rep.* **2017**, *7* (1), 408. https://doi.org/10.1038/s41598-017-00298-2.

(30) Völgyi, B. Molecular Biology of Retinal Ganglion Cells. *Cells* **2020**, *9* (11), 2483. https://doi.org/10.3390/cells9112483.

(31) Pan, T.; Shen, H.; Yuan, S.; Lu, G.; Zhang, Y.; Wang, H.; Zhao, Y.; Sun, X.; Liu, Q. Combined Transplantation With Human Mesenchymal Stem Cells Improves Retinal Rescue Effect of Human Fetal RPE Cells in Retinal Degeneration Mouse Model. *Investig. Opthalmology Vis. Sci.* **2020**, *61* (8), 9. https://doi.org/10.1167/iovs.61.8.9.

(32) Takagi, S.; Mandai, M.; Gocho, K.; Hirami, Y.; Yamamoto, M.; Fujihara, M.; Sugita, S.; Kurimoto, Y.; Takahashi, M. Evaluation of Transplanted Autologous Induced Pluripotent Stem Cell-Derived Retinal Pigment Epithelium in Exudative Age-Related Macular Degeneration. *Ophthalmol. Retina* **2019**, *3* (10), 850–859. https://doi.org/10.1016/j.oret.2019.04.021.

(33) Barber, A. J.; Lieth, E.; Khin, S. A.; Antonetti, D. A.; Buchanan, A. G.; Gardner, T. W. Neural Apoptosis in the Retina during Experimental and Human Diabetes. Early Onset and Effect of Insulin. *J. Clin. Invest.* **1998**, *102* (4), 783–791. https://doi.org/10.1172/JCI2425.

(34) Barber, A. J.; Antonetti, D. A.; Gardner, T. W. Altered Expression of Retinal Occludin and Glial Fibrillary Acidic Protein in Experimental Diabetes. **2000**, *41* (11), 8.

(35) Miller, J. W.; Adamis, A. P.; Aiello, L. P. Vascular Endothelial Growth Factor in Ocular Neovascularization and Proliferative Diabetic Retinopathy. **1997**, 14.

(36) Rossino, M. G.; Lulli, M.; Amato, R.; Cammalleri, M.; Dal Monte, M.; Casini, G. Oxidative Stress Induces a VEGF Autocrine Loop in the Retina: Relevance for Diabetic Retinopathy. *Cells* **2020**, *9* (6), 1452. https://doi.org/10.3390/cells9061452.

(37) Fu, Y.; Yau, K.-W. Phototransduction in Mouse Rods and Cones. *Pflüg. Arch. - Eur. J. Physiol.* **2007**, *454* (5), 805–819. https://doi.org/10.1007/s00424-006-0194-y.

(38) Lenahan, C.; Sanghavi, R.; Huang, L.; Zhang, J. H. Rhodopsin: A Potential Biomarker for Neurodegenerative Diseases. *Front. Neurosci.* **2020**, *14*, 326. https://doi.org/10.3389/fnins.2020.00326.

(39) The Retinal Pigment Epithelium in Visual Function | Physiological Reviews https://journals.physiology.org/doi/full/10.1152/physrev.00021.2004?rfr_dat=cr_pub++0pubmed&url_ver=Z39.88-2003&rfr_id=ori%3Arid%3Acrossref.org (accessed Jan 4, 2021).

(40) Kim, J. M.; Hong, K.-S.; Song, W. K.; Bae, D.; Hwang, I.-K.; Kim, J. S.; Chung, H.-M. Perivascular Progenitor Cells Derived From Human Embryonic Stem Cells Exhibit Functional Characteristics of Pericytes and Improve the Retinal Vasculature in a Rodent Model of Diabetic Retinopathy. *STEM CELLS Transl. Med.* **2016**, *5* (9), 1268–1276. https://doi.org/10.5966/sctm.2015-0342.

(41) Yang, J.; Cai, B.; Glencer, P.; Li, Z.; Zhang, X.; Li, X. Induced Pluripotent Stem Cells and Outer Retinal Disease. *Stem Cells Int.* **2016**, *2016*, 1–6. https://doi.org/10.1155/2016/2850873.

(42) Nehls, V.; Drenckhahn, D. Heterogeneity of Microvascular Pericytes for Smooth Muscle Type Alpha-Actin. *J. Cell Biol.* **1991**, *113* (1), 147–154. https://doi.org/10.1083/jcb.113.1.147.

(43) Hamilton, N. B. Pericyte-Mediated Regulation of Capillary Diameter: A Component of Neurovascular Coupling in Health and Disease. *Front. Neuroenergetics* **2010**, *2*. https://doi.org/10.3389/fnene.2010.00005.

(44) MacVicar, B. A.; Newman, E. A. Astrocyte Regulation of Blood Flow in the Brain. *Cold Spring Harb. Perspect. Biol.* **2015**, *7* (5), a020388. https://doi.org/10.1101/cshperspect.a020388.

(45) A Perivascular Origin for Mesenchymal Stem Cells in Multiple Human Organs: Cell Stem Cell https://www.cell.com/cell-stem-cell/fulltext/S1934-5909(08)00337-8?_returnURL=https%3A%2F%2Flinkinghub.elsevier.com%2Fretrieve%2Fpii%2FS1934590908003378%3Fshowall%3Dtrue (accessed Jan 10, 2021).

(46) Wittig, D.; Jászai, J.; Corbeil, D.; Funk, R. H. W. Immunohistochemical Localization and Characterization of Putative Mesenchymal Stem Cell Markers in the Retinal Capillary Network of Rodents. *Cells Tissues Organs* **2013**, *197* (5), 344–359. https://doi.org/10.1159/000346661.

(47) Pericytes at the intersection between tissue regeneration and pathology https://www.ncbi.nlm.nih.gov/pmc/articles/PMC4200531/ (accessed Jan 10, 2021).

(48) Carvalho, K. A. T.; Guarita-Souza, L. C.; Hansen, P.; Rebelatto, C. L. K.; Senegaglia, A. C.; Miyague, N.; Olandoski, M.; Francisco, J. C.; Furuta, M.; Gremski, W. Cell Transplantation After The Coculture of Skeletal Myoblasts and Mesenchymal Stem Cells in the Regeneration of the Myocardium Scar: An Experimental Study in Rats. *Transplant. Proc.* **2006**, *38* (5), 1596–1602. https://doi.org/10.1016/j.transproceed.2006.03.023.

(49) IJMS | Free Full-Text | Adult Stem Cell Therapeutics in Diabetic Retinopathy | HTML https://www.mdpi.com/1422-0067/20/19/4876/htm#B29-ijms-20-04876 (accessed Jan 10, 2021).